

## Diffusion Aspects in the Crystallization of Isotactic Polystyrene from Solutions

Takashi Sasaki,<sup>\*,†</sup> Masao Kurita, Tomoyoshi Yabu, and Toshisada Takahashi

Department of Materials Science & Engineering, Fukui University, 3-9-1 Bunkyo, Fukui 910, Japan

Received April 17, 1995; Revised Manuscript Received September 6, 1995<sup>®</sup>

**ABSTRACT:** Isothermal crystallization rates of isotactic polystyrene from tripropionin (TP), dimethyl sulfoxide (DMSO), and dimethyl phthalate (DMP) solutions were investigated by differential calorimetric measurements. The overall crystallization rate in the DMP solution exhibited a maximum at ca. 70 °C, which indicates that the diffusion factor plays an important role in the solution crystallization. The observed temperature dependence of the isothermal crystallization rate was analyzed on the basis of the Fokker–Planck type formula for the diffusion factor. The frictional interaction between the polymer and solvent was estimated, and the result showed that the diffusion processes (molecular motions) in the solution crystallization do not belong to the diffusion limit of Kramers. This fact has been expected for the solution crystallization, in which the frictional interaction between the polymer and solvent is weak. It has also been shown that the above tendency is remarkably dependent on the solvent. The frictional interaction was qualitatively evaluated to be DMP > DMSO > TP.

### Introduction

The crystallization of polymers is a fascinating subject for many researchers in the field of polymer science because of its specific feature including non-equilibrium processes.<sup>1</sup> The chain-folding feature can be explained by the idea that polymer crystallization is essentially a kinetics-controlled process with surface nucleation.<sup>2–5</sup> However, the precise picture of the polymer crystallization mechanism is still unknown in spite of a number of studies on the subject.<sup>6</sup> The rate of polymer crystallization is usually affected by two factors, namely, the thermodynamic driving force, which is referred to as the entropy factor  $G_e$ , and the transportation (molecular motions) of the polymer chain, which is referred to as the diffusion factor  $G_d$ , in the formula of crystallization rate. The crystallization rate  $G$  is expressed as  $G = G_0 G_e G_d$ , where  $G_0$  is the pre-exponential factor.  $G_e$  increases with increasing supercooling, and  $G_d$  increases with increasing absolute temperature. Hence, in general, the polymer crystallization rate under an isothermal condition exhibits a maximum at a certain temperature (supercooling). Indeed, this feature has usually been found for the melt crystallization. As for crystallization from solutions (solution crystallization), however, most of the studies have reported monotonous increasing crystallization rates with increasing supercooling.<sup>7–11</sup> These data have been frequently treated without taking into account the diffusion factor. To our knowledge, only a few papers<sup>12–14</sup> to date have reported the existence of the maximum for the solution crystallization of polymers.

It is unrealistic, however, to consider that the diffusion factor can be neglected for the solution crystallization. We now attribute this singularity of solution crystallization that does not exhibit the maximum, to the low-friction feature of the diffusion process, as described in the next section. The purpose of the present study is to ascertain the validity of our assumption and to evaluate the frictional aspect of the diffusion

process in the solution crystallization from different solvents. We employ isotactic polystyrene (iPS) as a typical crystallizable polymer, which has been reported to show the maximum for the rate of solution crystallization in certain solvents at high supercoolings.<sup>13,14</sup> The overall rate of isothermal crystallization from solutions is examined using differential scanning calorimetry (DSC) at various temperatures. Tripropionin (glycerol tripropionate, referred to as TP), dimethyl sulfoxide (DMSO), and dimethyl phthalate (DMP) are used as solvents.

### Diffusion Aspect Based on the Reaction Rate Theory

In this section, we show how the diffusion aspect influences the profile of the crystallization rate with respect to the crystallization temperature based on the reaction rate theory of barrier crossing for the diffusion process. In the solution crystallization process, the interaction between the polymer and solvent plays an important role. In the diffusion process concerning polymer chain dynamics, such polymer-solvent interaction may be interpreted as the degree of friction. According to the reaction rate theory of Kramers,<sup>15,16</sup> if the friction between the polymer and solvent molecules is extremely high (diffusion limit), the temperature dependence of the diffusion rate is influenced by a sum of the activation energy of the polymer elementary motion of diffusion  $E_a$  and that of solvent viscosity  $E_\eta$  as

$$G_d = \exp[-(E_a + E_\eta)/RT] \quad (1)$$

where  $R$  is the gas constant. On the other hand, if the friction between the polymer and solvent molecules is extremely low (low-friction limit), the solvent viscosity does not affect the polymer diffusion process, namely,

$$G_d = \exp(-E_a/RT) \quad (2)$$

For the intermediate region between the above two limiting cases, the diffusion rate is expressed by the so-called Fokker–Planck type formula as<sup>17</sup>

<sup>†</sup> Tel: 0776-27-8791. Fax: 0776-27-8767.

<sup>®</sup> Abstract published in *Advance ACS Abstracts*, November 1, 1995.

$$G_d = \exp[-(E_a + E_\eta)/RT] / \{0.5 + [0.25 + A_1 \exp(-2E_\eta/RT)]^{0.5}\} \quad (3)$$

where  $A_1$  is a parameter relative to the profile of the potential barrier for the elementary motion of the polymer diffusion. Note that  $A_1 = 0$  corresponds to the diffusion limit.

Now, it is pertinent to suppose that the polymer diffusion process in the solution crystallization occurs in the region near the low-friction limit, because the polymer is essentially insoluble in the solvent during the solution crystallization process; thus the frictional interaction between the polymer and solvent may be rather weak. This assumption explains the singularity of solution crystallization as described below.

We now show in Figure 1 the crystallization rates that are theoretically calculated for the above two limiting cases of the diffusion aspect. Here, we use the system of iPS in TP ( $E_\eta = 6.5 \text{ kcal mol}^{-1}$ ) as an example, assuming that  $E_a = 1.9$  and  $5.0 \text{ kcal mol}^{-1}$ . The entropy factor  $G_e$  of the crystallization rate can be expressed on the basis of the kinetics theory of the surface nucleation for the chain folding as<sup>2-5</sup>

$$G_e = \exp\left(-\frac{K_g T_d^\circ}{T \Delta T}\right) \quad (4)$$

with

$$K_g = \frac{x b \sigma \sigma_e}{k \Delta H} \quad (5)$$

where  $T_d^\circ$  is the equilibrium dissolution temperature,  $\Delta T$  is the supercooling ( $\Delta T = T_d^\circ - T$ ),  $x$  is a number that depends on the regime of the surface nucleation,  $b$  is the thickness of a stem,  $\sigma$  is the lateral surface free energy,  $\sigma_e$  is the fold surface free energy,  $k$  is the Boltzmann constant, and  $\Delta H$  is the polymer heat of dissolution. In the calculation for Figure 1, we use the value of  $232 \text{ deg}$  for  $K_g$ , which was obtained from the melt crystallization study of iPS,<sup>18</sup> and the value of  $180^\circ\text{C}$  for  $T_d^\circ$ , which was experimentally determined in this study, as will be described later.

Evidently, we can see in Figure 1 that the maximum appears at higher supercoolings for the low-friction limit than for the diffusion limit. In practice, the precipitation (phase separation) from solution tends to dominate the crystallization process at such higher supercoolings; therefore, the maximum may not be detected. Thus, the reason for the absence of the maximum in the solution crystallization data is possibly attributed to the diffusion aspect associated with the low friction between the polymer and solvent.

## Experimental Section

Commercial iPS (Scientific Polymer Products, Inc.,  $M_w = 4 \times 10^5$ ; triad tacticity, 90% isotactic) was used without further purification. The polymer was dissolved in TP, DMSO, and DMP with stirring for 15 min at 220, 188, and 220  $^\circ\text{C}$ , respectively, and we obtained completely homogeneous solutions. The concentrations of the solutions were made to be 5 wt %. The obtained solution was quenched at the crystallization temperature, and a small amount was then removed from the solution at the appropriate times, which was immediately quenched in a liquid  $\text{N}_2$  bath. The polymer thus removed was then precipitated in methanol and was washed several times with methanol. Finally, it was dried in a vacuum desiccator for 15 h, and the DSC measurements were taken to determine the extent of crystallization.

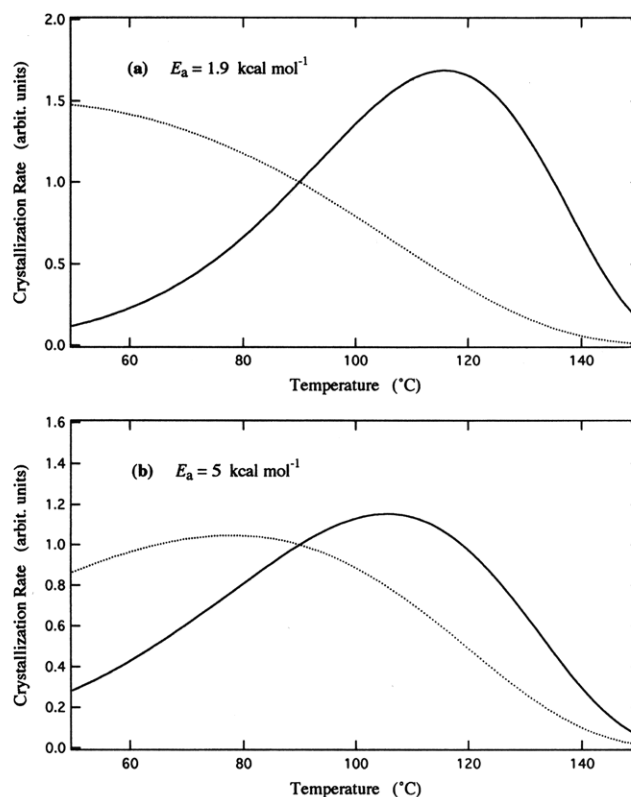


**Figure 1.** Theoretical isothermal crystallization rate calculated for the diffusion limit (solid line) and low-friction limit (dotted line).

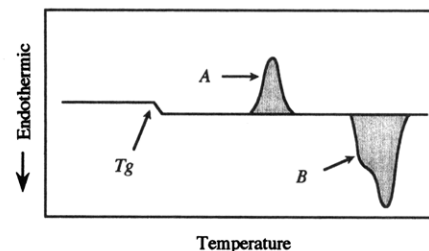


**Figure 2.** Schematic representation of a typically observed DSC thermogram. The area A of the exothermic peak represents the heat of crystallization during the DSC measurement, and the area B of the endothermic peak represents the heat of fusion of the totally crystallized fraction.

The DSC measurements were carried out at a heating rate of  $5^\circ\text{C min}^{-1}$  in air with a Seiko DSC 200 apparatus equipped with a thermal analysis station SSC-4000. The temperature readings were calibrated with an indium standard. Figure 2 shows a schematic of a typical thermogram. The peak area A in this figure represents the heat of crystallization during the DSC measurement, and B represents the heat of fusion of the total crystallized fraction. Thus,  $B - A$  is the heat of fusion of the crystalline fraction formed in the isothermal solution crystallization. We evaluated the extent of crystallization  $f_c(t)$  as

$$f_c(t) = (B - A)/B \quad (6)$$

The overall crystallization (crystal growth) rate  $G$  was estimated with a reciprocal of the half-time for reaching the final value of crystallinity, i.e.,  $G = 1/t_{0.5}$ .

The obtained data for the crystallization rate with respect to the crystallization temperature were analyzed by fitting with the formula  $G = G_0 G_e G_d$ , with eqs 3 and 4. We executed the fitting procedure by the nonlinear least squares method of the modified Marquardt algorithm,  $E_a$ ,  $\ln A_1$ , and  $K_g$  being treated as variable parameters.

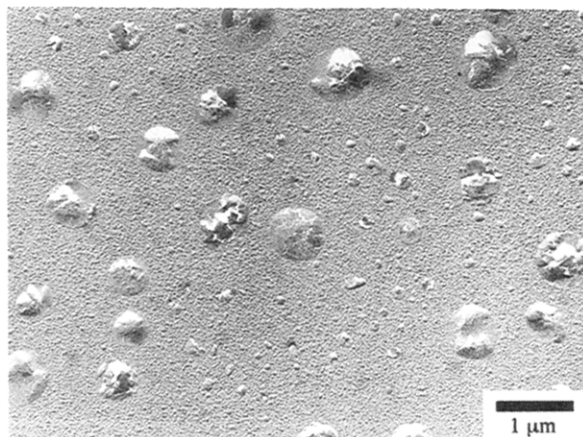


**Figure 3.** Transmission electron micrograph of the precipitant crystallized at 100 °C from TP.

To determine the equilibrium dissolution temperature  $T_d^\circ$ , which was needed for the data analysis, a 5 wt % DMP solution of iPS was prepared at 220 °C, and it was then quenched in a liquid  $N_2$  bath to obtain completely amorphous iPS. The obtained precipitant was washed in methanol, dried under a vacuum, and annealed at several temperatures to obtain the samples of different lamellar thicknesses  $l$ . The melting temperatures  $T_m$  and dissolution temperatures  $T_d$  of each solvent at 10 wt % of these annealed samples were measured by DSC. Finally, we determined the equilibrium dissolution temperature by an extrapolation to  $l^{-1} = 0$  according to the relations<sup>5</sup>

$$l = \frac{2\sigma_e T_m^\circ}{\Delta H(T_m^\circ - T_m)} \quad (7)$$

$$T_d = T_d^\circ \left(1 - \frac{2\sigma_e}{\Delta Hl}\right) \quad (8)$$

where  $T_m^\circ = 242$  °C (equilibrium melting point),  $\Delta H = 91.1$  J  $cm^{-3}$ , and  $\sigma_e = 28.8 \times 10^{-7}$  J  $cm^{-2}$ .<sup>18,19</sup> The obtained  $T_d^\circ$ 's were 180 °C for TP and 195 °C for DMSO. For DMP, we used a value 201 °C from the literature.<sup>14</sup> The activation energies of viscosity  $E_\eta$  of the solvents were determined to be 6.5 kcal  $mol^{-1}$  for TP, 3.03 kcal  $mol^{-1}$  for DMSO, and 6.11 kcal  $mol^{-1}$  for DMP by viscosity measurements with an Ubbelohde type viscometer.

The morphology of the iPS crystals was examined by a transmission electron microscope (TEM) (JEOL Datum JEM-2000FXII) equipped with a scanning electron microscope (SEM) (EM-ASID20). We prepared the samples for observation by depositing the turbid solutions that were obtained after the isothermal crystallization had proceeded to completion onto Cu meshes covered with cellulose nitrate membranes. The sample meshes were shadowed with Au before the observations were taken.

We also evaluated the chain conformation in the solutions by Fourier-transform infrared (FT-IR) spectroscopy. The samples for measurement were prepared as follows: the solutions of the three solvents prepared in the same procedure mentioned above were rapidly frozen in a liquid  $N_2$  bath, and the solvents were immediately extracted from the frozen solutions with methanol at  $-45$  °C for DMSO and DMP and at  $-90$  °C for TP. At these temperatures the polymer conformations are considered to be frozen (well below  $T_g$ ). The remaining polymers were then washed with methanol several times and were dried in vacuum. The content of the helical structure of these sample polymers was evaluated by an FT-IR spectrometer (Perkin-Elmer Paragon 1000).

## Results and Discussion

**Morphology.** Figure 3 shows a transmission electron micrograph of the crystallized precipitant from the

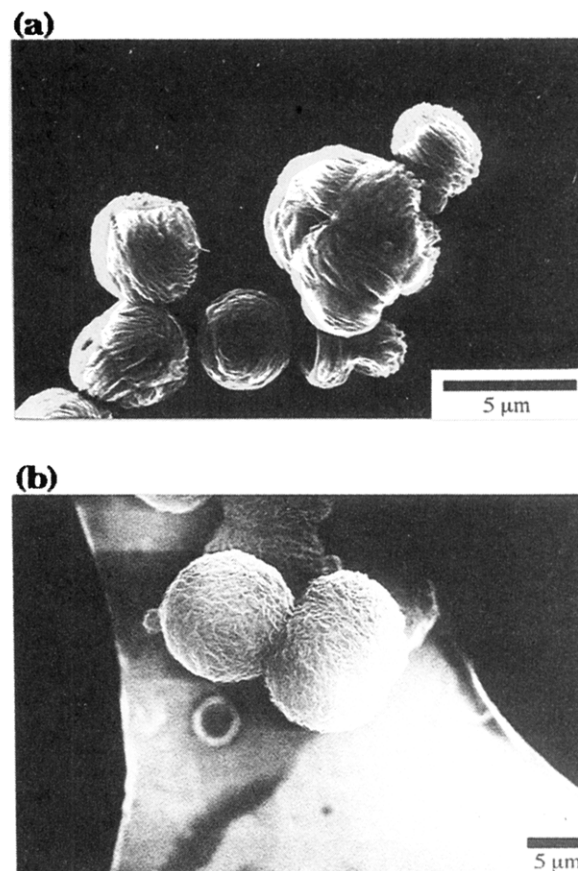


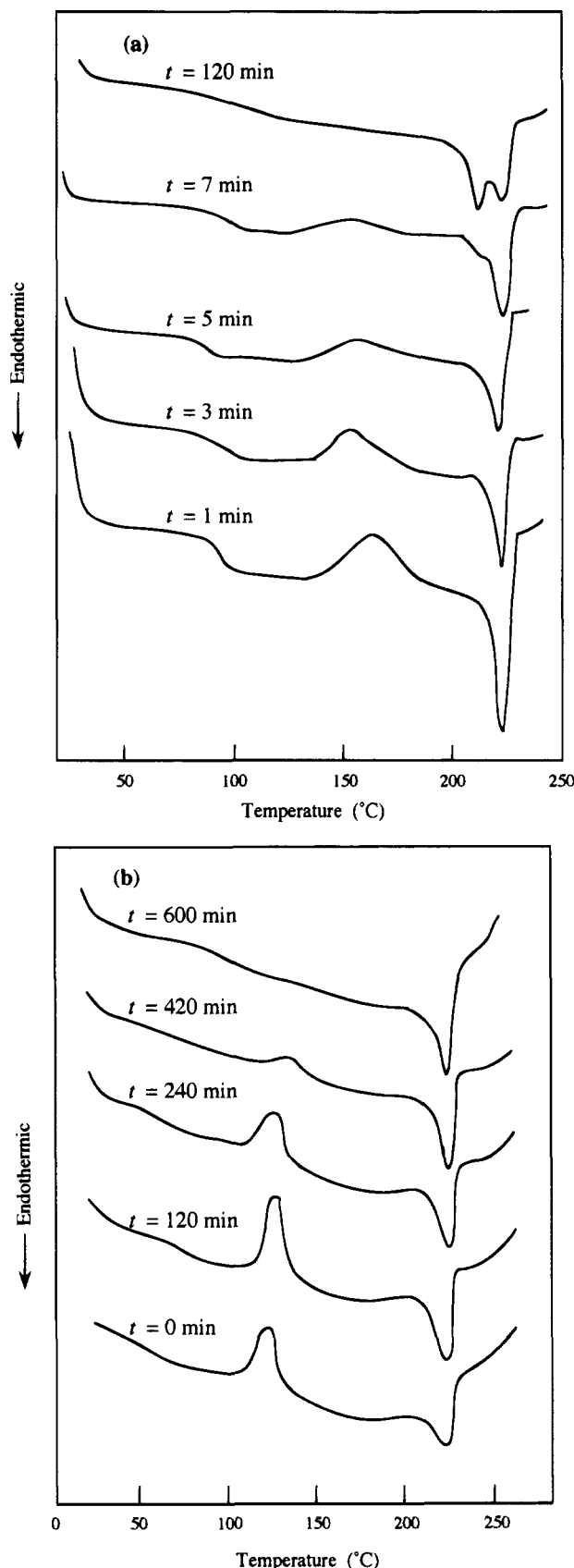
**Figure 4.** Scanning electron micrographs of the precipitants crystallized from (a) DMSO and (b) DMP solutions at 140 and 63 °C, respectively.

TP solution. The shape of crystal observed here is similar to that observed by Tanzawa in dilute (0.1%) DMP solution at high supercoolings,<sup>14</sup> i.e., rounded circles (probably deformed hexagons) with diameters of about 0.5–1  $\mu m$  were obtained. The same morphology was observed throughout the temperature region of our study for the TP solution (90–150 °C), which suggests that the regime transition does not seem to occur.

Figure 4 shows the scanning electron micrographs of crystals obtained from DMSO and DMP solutions. In these cases, sphere-like crystalline particles of larger sizes (5–10  $\mu m$ ) were observed. As the observed crystals grown from these two solvents were not revealed to be spherulites by polarizing optical microscopy, the sphere-like particles may be composed of a number of aggregated crystallites such as small hedrites. The aggregation probably occurred when the solution was cooled to room temperature after the solution crystallization was completed.

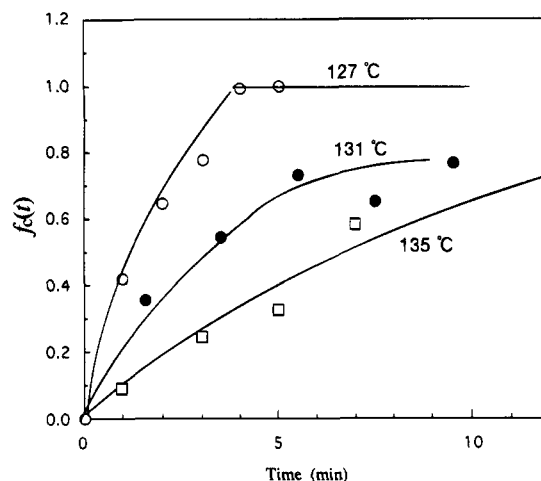
**Results of the DSC Measurements.** In the course of solution crystallization, no gelation was recognized in DMSO and DMP in the present temperature ranges (123–151 °C for DMSO and 50–90 °C for DMP), whereas, apparent gelation was occasionally observed in TP when the initial dissolution was accidentally incomplete. In such a case, two endothermic peaks appeared at about 50 and 120 °C in the DSC data, which are relevant to the gel melting.<sup>13</sup> We discarded these data associated with the gelation.

Figure 5 shows the typical DSC results obtained during the crystallization process in DMSO and DMP, which indicate no signs of gelation. It was confirmed for every measurement that the peak area A is equal



**Figure 5.** DSC thermograms of the samples obtained after various times of isothermal crystallization  $t$  from (a) DMSO solution at 135 °C and (b) DMP solution at 65 °C. The measurements were carried out at a heating rate of 5 °C min<sup>-1</sup>. The exothermic peak decreases with time as the isothermal crystallization proceeds.

to B at  $t = 0$ . This implies that the polymer had been completely dissolved in the solvent and that no extra



**Figure 6.** Time development of the extent of crystallization  $f_c(t)$  from DMSO at the crystallization temperatures 127, 131, and 135 °C.

crystallization had occurred during the liquid N<sub>2</sub> quenching, methanol washing, and drying under a vacuum. Thus, we made sure of the validity of the experiment.

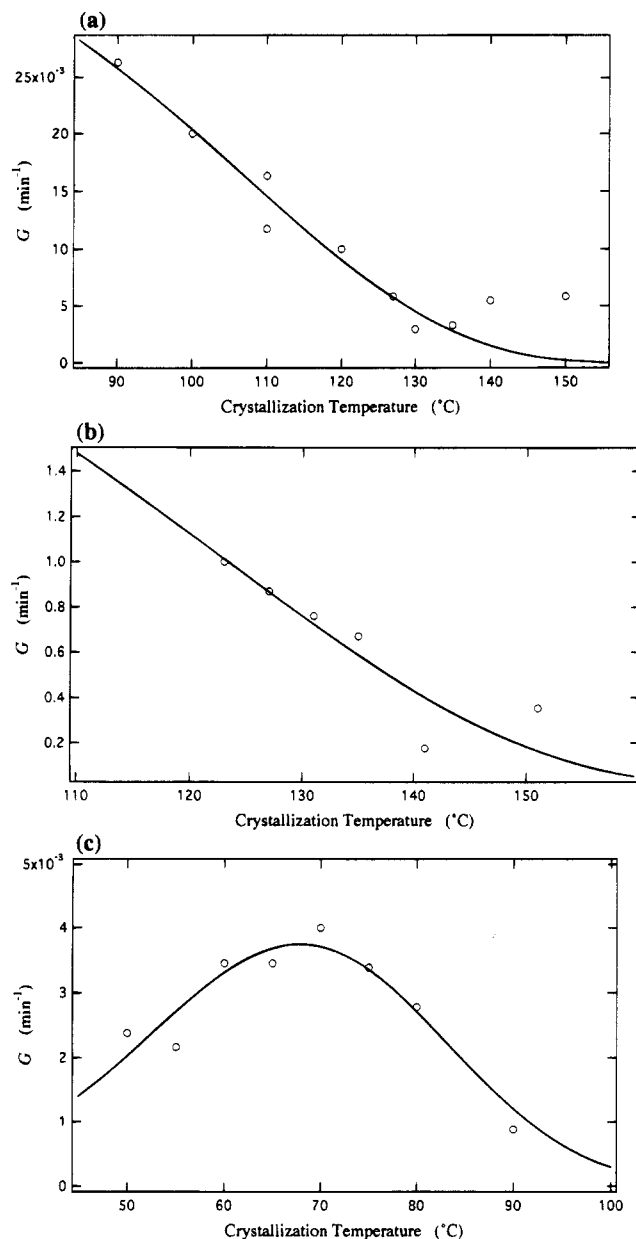
**Crystallization Rate.** Figure 6 shows examples of the time dependence of the extent of crystallization  $f_c(t)$  from DMSO solutions. Figure 7 shows the rate of crystallization  $G$  (reciprocal of half-time for reaching the final value of crystallinity) with respect to the crystallization temperature. For the TP and DMSO solutions,  $G$  monotonously decreases with increasing temperature. On the other hand, in DMP, a maximum appears at a rather high supercooling ( $\Delta T \approx 130$  K). A similar result has also been reported for a DMP solution at a lower concentration (0.1%) by the measurement of the radial growth rate.<sup>14</sup> The existence of the maximum can be interpreted as the contribution of the diffusion factor; i.e., we should not neglect the transportation effect of the polymer chain (diffusion factor) even in the solution crystallization.

Table 1 shows the parameters obtained from the analysis of the  $G$  vs  $T$  data for the three solutions together with the other parameters used in the analysis. We plotted the fitted curves obtained from the present analysis with solid lines in Figure 7. To evaluate the contribution of solvent viscosity to the crystallization rate, we introduce a parameter  $\alpha$  defined as

$$\alpha = \frac{2\sqrt{A_1} \exp(-E_f/RT)}{2\sqrt{A_1} \exp(-E_f/RT) + 1} \quad (9)$$

When  $\alpha = 0$ , the diffusion process belongs to the diffusion limit of Kramers (i.e., the frictional interaction is extremely strong), and when  $\alpha = 1$ , the diffusion process belongs to the low-friction limit. It is readily seen from eq 9 that  $\alpha$  depends on temperature; therefore, the values listed in Table 1 indicate the ranges that correspond to the temperature ranges of our experiments.

The result in Table 1 shows that in the present temperature ranges the diffusion limit is not feasible for all the three solutions investigated. The obtained  $\alpha$  reveals that the diffusion aspect is in the low-friction limit ( $\alpha = 1$ ) for the TP solution, in the vicinity of the low-friction limit for the DMSO solution, and in the intermediate region between the two limits for the DMP solution. Thus, it is shown that the strength of the frictional interaction between the polymer and solvent



**Figure 7.** Isothermal crystallization rate with respect to crystallization temperature for (a) TP, (b) DMSO, and (c) DMP solutions. The solid lines indicate the fitted curves calculated with the parameters in Table 1.

**Table 1.** Obtained Parameters for the Crystallization Rate from the Three Solutions

|                                    | solvent               |                    |                       |
|------------------------------------|-----------------------|--------------------|-----------------------|
|                                    | TP                    | DMSO               | DMP                   |
| temp range (K)                     | 363–423               | 396–424            | 323–363               |
| $E_a$ (kcal mol <sup>-1</sup> )    | 1.85                  | 1.79               | 31.8                  |
| $K_g$ (deg)                        | 222                   | 225                | $3.26 \times 10^3$    |
| $\alpha$                           | 1                     | 0.884–0.908        | 0.322–0.575           |
| $G_0$ (min <sup>-1</sup> )         | $2.52 \times 10^{20}$ | $8.09 \times 10^4$ | $6.03 \times 10^{36}$ |
| $E_\eta$ (kcal mol <sup>-1</sup> ) | 6.5                   | 3.03               | 6.11                  |

is DMP > DMSO > TP solutions. As for the TP solution, the obtained value of the polymer activation energy 1.85 kcal mol<sup>-1</sup> with  $\alpha = 1$  (low-friction limit), which is even smaller than  $E_\eta$  (6.5 kcal mol<sup>-1</sup>), undoubtedly indicates the invalidity of the diffusion limit, implying an unrealistic negative activation energy in the case of the diffusion limit (–4.65 kcal mol<sup>-1</sup>). One of the authors has already reported that the diffusion limit is invalid even in the equilibrium TP solution of

**Table 2.** Relative Absorbance of the Helical Bands for the iPS Extracted from the Solutions

|  | solvent |      |      | ref <sup>a</sup> |
|--|---------|------|------|------------------|
|  | TP      | DMSO | DMP  |                  |
| $A(565 \text{ cm}^{-1})/A(1601 \text{ cm}^{-1})$ | 0.68    | 0.76 | 0.61 | 1.06             |
| $A(586 \text{ cm}^{-1})/A(1601 \text{ cm}^{-1})$ | 0.17    | 0.27 | 0.11 | 0.48             |

<sup>a</sup> iPS crystallized from a 5 wt % DMP solution at 70 °C for 10 h.

atactic polystyrene.<sup>20,21</sup> This may be consistent with the present result of the small frictional interaction in the TP solution.

The present results for the TP and DMSO solutions do not show a maximum in the  $G$  vs  $T$  plots. This is due to the fact that the manner of the polymer–solvent interaction is far from the diffusion limit of Kramers in these two solvents and in that case, the temperature for the maximum growth rate is lowered. In practice, we could not investigate the solution crystallization at higher supercoolings below the present temperature ranges for the TP and DMSO solutions, because the deposition of the polymer (phase separation) occurred much more rapidly than the crystallization process. Strictly speaking, the *solution crystallization*, in that the phase separation and the crystallization must simultaneously occur, was not accomplished at the higher supercoolings.

**Chain Conformation of iPS in Solutions.** It is now essential to examine the chain conformation of iPS in the present solutions, because it may strongly influence the mechanism and consequently the rate of solution crystallization. The existence of the  $3_1$  helical structure even in equilibrium solutions of certain solvents has been reported.<sup>22–25</sup> In such a case, the crystallization process is merely the aggregation of already existing helices in the solution, and the crystallization occurs easily with no need for the helix formation. We evaluated the conformation of iPS in the solutions by FT-IR spectroscopy, as described in the Experimental Section. The result showed that for all the three solutions no apparent absorption peak was observed at 586.5 and 557.5 cm<sup>-1</sup>, where the absorption bands due to the isotactic helical conformation should appear.<sup>24,26</sup> Table 2 shows the absorbance at these two frequencies relative to the absorbance due to the phenyl ring vibrations at 1601 cm<sup>-1</sup>. The data for the iPS crystallized from the DMP solution at 70 °C for 10 h are also listed as a reference. It is thus revealed that the iPS dissolved in the present three solvents tends to assume a random coil structure without the  $3_1$  helical conformation and that the crystallization from the present solutions contains the formation of the helical structure. Since this tendency is observed for all three solvents, the difference in the crystallization rate between the three solutions can mainly be attributed to the difference in the aspect of the polymer–solvent interactions.

**Activation Energy.** The activation energies for the polymer motions  $E_a$  listed in Table 1 are dependent on the solvent;  $E_a$  seems to decrease as the diffusion aspect approaches the low-friction limit. This may suggest that the mode of molecular motions dominant in the crystallization process is different among the three solvents, i.e., larger modes of motions become dominant with increasing frictional interaction, provided that the larger motions are associated with higher barriers. However, the value of 31.8 kcal mol<sup>-1</sup> obtained for the DMP solution may be too large compared with that for the

**Table 3. Comparison of the Crystallization Rate at  $\Delta T = 100$  K**

|                                | TP     | DMSO | DMP                   |
|--------------------------------|--------|------|-----------------------|
| $G_{100}$ (min <sup>-1</sup> ) | 0.0203 | 1.87 | $2.94 \times 10^{-4}$ |

TP solution, 1.85 kcal mol<sup>-1</sup>. The latter value is consistent with the value of 1.9 kcal mol<sup>-1</sup> obtained for atactic polystyrene in a dilute TP solution by the fluorescence method.<sup>20</sup> The large activation energy for the DMP solution may be due to the singularity characteristic to the polymer chain dynamics under a nonequilibrium condition of the solution crystallization and may also be due to the invalidity of the nucleation-controlled growth mechanism, as mentioned below.

**Entropy Factor.** The obtained values of the entropy parameter  $K_g$  for the DMSO and TP solutions are similar to that for the melt crystallization (232 deg).<sup>18</sup> This may indicate that the free energy of the iPS in our solutions is similar to that of the melt state. Indeed, the present concentration (5 wt %) is high enough for the iPS chains of  $M_w = 4 \times 10^5$  to overlap each other, and in such a case, the chain expansion may be reduced as the excluded volume effect is screened and, as a result, approaches to some extent that of the melt state ( $\Theta$  condition).

For the DMP solution, on the other hand, we could not find a reasonably fitted curve with  $K_g \approx 232$  deg: the obtained value is  $3.26 \times 10^3$  deg (Table 1). This is extremely large compared with the literature value for the melt crystallization. For the crystallization from a dilute DMP solution (0.1 wt %), a larger value has also been reported (958 deg),<sup>14</sup> but the present result is even larger than this. The inconsistency may be due to the different concentration and also to the different experimental method.

In any case, the present result shows that  $K_g$  is larger for the solution crystallization from DMP than for the melt crystallization. This indicates a larger surface free energy and/or a smaller  $\Delta H$  for the solution crystallization in terms of the nucleation theory. One possible explanation for this phenomenon is that the crystal growth is not controlled by the usual surface nucleation process in the case of the DMP solution at high supercoolings. Indeed, the number of stems in a critical nucleus is far below 1 in the present temperature range for the DMP solution, which means that the usual nucleation theory is invalid.<sup>14</sup> It has also been reported that the long spacing of iPS crystallized from a DMP solution exhibits a constant lowest value at high supercoolings,<sup>25</sup> which conflicts with the surface nucleation theory. Thus, an alternative growth mechanism is to be established for the present system at high supercoolings. However, we will not discuss this fascinating but cumbersome problem further, because our main interest is concentrated on the diffusion process, and the problem appears to be beyond our scope.

**Comparison of the Absolute Value of  $G$ .** We also found that the absolute value of  $G$  strongly depends on the solvent. Table 3 shows the values of  $G_{100}$ , the crystallization rate at a supercooling  $\Delta T = 100$  K, for comparison. We can see that  $G_{100}(\text{DMSO}) > G_{100}(\text{TP}) > G_{100}(\text{DMP})$ . Such solvent dependence is not merely due to the difference in viscosity: the solvent viscosity is 0.437–0.564 cP for DMSO, 0.198–0.712 cP for TP, and 2.72–7.77 cP for DMP in our experimental temperature ranges. There is also no qualitative correlation between the absolute value of  $G$  and the frictional interaction previously discussed. The order of magni-

tude of  $G$  is rather dominated by the solubility (compatibility) of the polymer to the solvent. Though the present three solvents do not dissolve iPS at the present experimental temperatures, the difference in the extent of the insolubility among the three solvents can be qualitatively evaluated. Worse solubility induces a stronger driving force for the phase separation and crystallization; thus, it increases the crystallization rate. Therefore, the above result implies that the solubility of iPS becomes larger in the order DMSO, TP, and DMP in the present temperature ranges.

## Conclusions

We have examined the dynamic feature in the crystallization of iPS from TP, DMSO, and DMP, by calorimetric measurements. In the  $G$  vs  $T$  plot for the DMP solution, a maximum point was observed, which means that the diffusion (transportation) factor should be taken into account. The temperature dependence of the diffusion factor in the crystallization rate was successfully analyzed by the Fokker–Planck type formula, which can treat a region from the diffusion (high-friction) limit to the low-friction limit. The obtained results revealed a difference in the frictional feature between the polymer and solvent among the three solvents studied. We have found that the polymer–solvent frictional interaction is largest for DMP and smallest for TP and that the absolute value of the crystallization rate is largest for DMSO and smallest for DMP.

The present results show that the diffusion factor in the crystallization rate plays an important role even in the solution crystallization in which a maximum in the  $G$  vs  $T$  plot is not apparently observed. The system of the solution crystallization is peculiar because of its small polymer–solvent frictional interaction, which cannot be accomplished in common equilibrium polymer solutions. Hence, the study of the polymer chain dynamics in such a specific circumstance is an interesting subject and they are to be scrutinized further in a wide variety of polymers and solvents.

**Acknowledgment.** This work was supported by a Grant-in-Aid for Scientific Research (No. 06855113) from the Ministry of Education, Science, and Culture, Japan.

## References and Notes

- (1) Mandelkern, L. *Crystallization of Polymers*; McGraw-Hill: New York, 1964.
- (2) Hoffman, J. D.; Lauritzen, J. I. *J. Res. Natl. Bur. Stands.* **1961**, 65A, 297.
- (3) Lauritzen, J. I.; Hoffman, J. D. *J. Appl. Phys.* **1973**, 44, 4340.
- (4) Lauritzen, J. I. *J. Appl. Phys.* **1973**, 44, 4353.
- (5) Armistead, K.; Goldbeck-Wood, G. *Adv. Polym. Sci.* **1992**, 100, 219.
- (6) See, for example: *Crystallization of Polymers*, NATO ASI-C Series; Dosièrè, M., Ed.; Kluwer: Dordrecht, The Netherlands, 1993.
- (7) Mandelkern, L. *J. Appl. Phys.* **1955**, 26, 443.
- (8) Sanchez, I. C.; DiMarzio, E. A. *Macromolecules* **1971**, 4, 677.
- (9) Keller, A.; Pedemonte, E. *J. Cryst. Growth* **1973**, 44, 111.
- (10) Cooper, M.; Manley, R. St. *J. Macromolecules* **1975**, 8, 219.
- (11) Toda, A.; Miyaji, H.; Kiho, H. *Polymer* **1986**, 27, 1505. Toda, A. *Ibid.* **1987**, 28, 1645.
- (12) Lemstra, P. J.; Challa, G. *J. Polym. Sci., Polym. Phys. Ed.* **1975**, 13, 1809.
- (13) Girolamo, M.; Keller, A.; Miyasaka, K.; Overbergh, N. *J. Polym. Sci., Polym. Phys. Ed.* **1976**, 14, 39.
- (14) Tanazawa, Y. *Polymer* **1992**, 33, 2659.

- (15) Kramers, H. A. *Physica* **1940**, 7, 284.
- (16) Hänggi, P.; Talkner, P.; Borkovec, M. *Rev. Mod. Phys.* **1990**, 62, 251.
- (17) Helfand, E. *J. Chem. Phys.* **1971**, 54, 4651.
- (18) Suzuki, T.; Kovacs, A. *Polym. J.* **1970**, 1, 82.
- (19) Edwards, B. C.; Phillips, P. J. *Polymer* **1974**, 15, 351.
- (20) Yokotsuka, S.; Okada, Y.; Tojo, Y.; Sasaki, T.; Yamamoto, M. *Polym. J.* **1991**, 23, 95.
- (21) Ono, K.; Okada, Y.; Yokotsuka, S.; Ito, S.; Yamamoto, M. *Polym. J.* **1994**, 26, 199.
- (22) Reiss, C.; Benoit, H. *J. Polym. Sci., Part C* **1968**, 16, 3079.
- (23) Keith, H. D.; Vadimsky, R. G.; Padden, J., Jr. *J. Polym. Sci., Polym. Chem. Ed.* **1970**, 8, 1687.
- (24) (a) Helms, J. B.; Challa, G. *J. Polym. Sci., Polym. Chem. Ed.* **1972**, 10, 761. (b) Helms, J. B.; Challa, G. *J. Polym. Sci., Polym. Chem. Ed.* **1972**, 10, 1447.
- (25) Jones, D. H.; Latham, A. J.; Keller, A.; Girolamo, M. *J. Polym. Sci., Polym. Phys. Ed.* **1973**, 11, 1759.
- (26) Painter, P. C.; Koenig, J. L. *J. Polym. Sci., Polym. Phys. Ed.* **1977**, 15, 1885.

MA950494Y